

Graphene is neither Relativistic nor Non-Relativistic case: Thermodynamics Aspects

Thandar Zaw Win, Cho Win Aung, Gaurav Khandal, Sabyasachi Ghosh
Indian Institute of Technology Bhilai, GEC Campus, Sejbahar, Raipur 492015, Chhattisgarh, India

Discovery of electron hydrodynamics in graphene system has opened a new scope of analytic calculations in condensed matter physics, which was traditionally well cultivated in science and engineering as a non-relativistic hydrodynamics and in high energy nuclear and astro physics as relativistic hydrodynamics. Electrons in graphene follow neither non-relativistic nor relativistic hydrodynamics and thermodynamics. Present article has gone through systematic microscopic calculations of thermodynamical quantities like pressure, energy density, etc. of electron-fluid in graphene and compared with corresponding estimations for non-relativistic and ultra-relativistic cases. Identifying the Dirac fluid and Fermi liquid domains, we have sketched the transition of temperature and Fermi energy dependency of electron thermodynamics for graphene and other cases. An equivalent transition for quark matter is also discussed. The most exciting part is the general expression of specific heat, whose Fermi to Dirac fluid domain transition can be realized as a transition from a solid-based to a fluid-based picture. This understanding may be connected to the experimentally observed Wiedemann-Franz Law violation in the Dirac fluid domain of graphene system.

I. INTRODUCTION

Fluid dynamics is a macroscopic theory to describe fluid motions in terms of space-time-dependent different densities like energy, momentum, number, etc. and widely well studied in the branch of applied mathematics, science and engineering [1]. When one enters into its microscopic physics, a non-relativistic kinetic theory appears for the matter of discussion [2, 3]. On the other hand, macroscopic and microscopic description of relativistic hydrodynamics [4, 5] is well developed and cultivated in high energy nuclear [4] and astro [5] physics. So, similar to non-relativistic hydrodynamics (NRHD) in the branches of applied mathematics, science and engineering [1], relativistic hydrodynamics (RHD) is also studied in a broad band of physics from High Energy Nuclear Physics [4] to Astro Physics [5] to String theory [6]. Interestingly, the hydrodynamics aspects never came into the picture in condensed matter physics or solid-state physics before the discovery of electron hydrodynamics (eHD) in graphene system (see Refs [7–9] for review). Due to the proportional relation between energy and momentum, electron motion in graphene will not be Galilean-invariant. On the other hand, the relativistic effect of electrons cannot also be expected, because its velocity is not very close to the speed of light. Hence, we can't claim the Lorentz-invariant property of electron motion. It opens "unconventional" hydrodynamics as neither non-relativistic nor relativistic hydrodynamics can be applicable. This hydrodynamic aspect in condensed matter physics is observed in some recent experimental works [10–27], which provide a challenge to the theoretical condensed matter physicists to comprehend these new aspects. It is graphene [10–22, 27], which is identified as the best known such material, where electron hydrodynamics has been nicely observed.

Apart from the recently discovered hydrodynamic aspect of graphene, there are some other famous properties of it, for which it constantly attracted the attention of the scientific community for a few decades from when it was discovered. See Ref. [28] for its quick review. Graphene [28] is a two-dimensional system of carbon atoms with some interesting properties like

1. zero band gap between the valance and conduction bands at Dirac points,
2. (effectively) zero mass behavior with proportional relation between electron's energy and momentum,

and many more interesting behaviors [28]. From the experimental point of view, this coincidence of gap-less and mass-less nature with the hydrodynamic aspects is an observed fact, but it was a theoretical challenge to find their inter-connection mechanism. According to the latest understanding [7–9], we may connect them by following links. Free electron theory of electron as Fermi gas is well applicable for most of the metals as they always have finite Fermi energy or chemical potential μ [29] within the range $\mu = 2 - 10$ eV. So only electrons on the Fermi-energy sphere will participate in the kinematics, thermodynamics, and transport phenomena. Other electrons, occupied below the Fermi energy sphere, will remain immobile due to the Pauli exclusion principle. So, (nearly) free electrons on the Fermi energy sphere will face obstacles of those immobile electrons as well as ions in real (co-ordinate) space (not in momentum space), for which zig-zag Ohmic type motions are followed by those free electrons. In other words, electron-electron scattering will be suppressed by other dominant scatterings like electron-ions and others, which can not be removed in this Ohmic type motion of Fermionic systems having large μ . These kinds of transportation provide internal energy density $\epsilon = a + bT^2$ and specific heat $c_V \propto T$ based on the Sommerfeld expansion calculation and also Wiedemann-Franz law is well obeyed. On the other hand, the picture may be changed for the graphene case, where μ can be decreased from the range $\mu = 2 - 10$ eV to smaller values (even towards $\mu \rightarrow 0$ limits) by changing

the doping level. So when one goes toward $\mu/T \ll 1$ domain, called Dirac fluid (DF) or Dirac liquid (DL), electron-electron scattering becomes dominating over other possible scatterings, and electron hydrodynamics or Poiseuille's motion is observed instead of Ohmic type motions. These kinds of fluid-based transportation may provide different expressions of internal energy density and may violate Wiedemann-Franz law [26]. Present article is aimed to explore the differences in thermodynamical properties for graphene case between $\mu/T \ll 1$ and $\mu/T \gg 1$ domains as well as compared with other cases like non-relativistic (NR) and ultra-relativistic (UR).

If we find the earlier references, then we will get Refs. [30–32], where graphene thermodynamics in the presence of magnetic field are studied. The correction term with non-interacting thermodynamics results is addressed in Refs [33, 34]. In this regard, the present work is only focused on non-interacting thermodynamics as well as no external magnetic field is considered. So, a straightforward statistical mechanical calculation will provide the information on graphene thermodynamics, which is basically addressed here, but we have stressed the comparison of thermodynamics for the graphene case to the other cases like NR and UR cases. Also, the transition of thermodynamics for those cases from 3 dimensions (3D) to 2 dimensions (2D) is documented. We have expressed our thermodynamical quantities like pressure P , energy density ϵ , specific heat c_V , number density n as functions of T and μ in terms of Fermi integral function

$$f_\nu(A) = \frac{1}{\Gamma(\nu)} \int_0^\infty \frac{x^{\nu-1}}{A^{-1}e^x + 1} dx \text{ (with } A = e^{\mu/k_B T} \text{)}. \quad (1)$$

After getting the general expressions of thermodynamics for all cases, we have explored their $\mu/T \gg 1$ limits by using Sommerfeld expansion and $\mu/T \ll 1$ or $\mu \rightarrow 0$ limits in terms of Riemann zeta function

$$\zeta_\nu = \frac{1}{\Gamma(\nu)} \int_0^\infty \frac{x^{\nu-1}}{e^x - 1} dx. \quad (2)$$

Through these comparative studies on thermodynamics, we want to zoom in on the fact that electrons of graphene system behave as neither non-relativistic nor relativistic cases, which is well known but sometimes misguided by the terminology - relativistic description of graphene. The present work demonstrates analytically as well as numerically the differences of graphene (G) case from NR and UR cases via different thermodynamical quantities. In parallel, it also shows that for some particular thermodynamical relations connected with the equation of state, G, and UR cases are hard to differentiate. It means that those thermodynamical outcomes may misguide us to think that electrons in graphene follow a relativistic description. This agenda is projected in this article with the organization - first formalism part in Sec. (II), then numerical results part in Sec. (III) and at the end, summary part in Sec. (IV).

II. FORMALISM

For any fluid description, we start with the energy-momentum tensor

$$T^{\mu\nu} = T_0^{\mu\nu} + T_D^{\mu\nu}, \quad (3)$$

where $T_0^{\mu\nu}$ is ideal part and $T_D^{\mu\nu}$ is dissipative part. For the present study, we will not concentrate on the dissipative part. In terms of the building blocks - energy density ϵ , pressure P , number density n , fluid four-velocity u^μ and metric tensor $g^{\mu\nu}$, we can write the ideal energy-momentum tensor and electron number flow as

$$\begin{aligned} T_0^{\mu\nu} &= \epsilon \frac{u^\mu u^\nu}{v_g^2} - P \left(g^{\mu\nu} - \frac{u^\mu u^\nu}{v_g^2} \right), \\ N_0^\mu &= n \frac{u^\mu}{v_g}. \end{aligned} \quad (4)$$

Here, one can design the four-velocity as $u^\mu = \gamma_g(v_g, \vec{u})$ for graphene hydrodynamic (GHD) by mapping the four-velocity structure $u^\mu = \gamma(c, \vec{u})$ for relativistic hydrodynamics (RHD), where speed of light c in RHD is basically replaced by electron Fermi velocity v_g in GHD. Corresponding Lorentz factor $\gamma = 1/\sqrt{1 - u^2/c^2}$ in RHD will also be changed to a modified factor $\gamma_g = 1/\sqrt{1 - u^2/v_g^2}$ in GHD. In static limit four-velocity, $u^\mu = \gamma_g(v_g, \vec{u})$ tends to $u^\mu = \gamma_g(v_g, \vec{0})$ and $\gamma_g = 1/\sqrt{1 - u^2/v_g^2}$ tends to 1. In this static limit, we will get $T_0^{00} = \epsilon$ and $T_0^{11} = T_0^{22} = T_0^{33} = P$, which is basically presenting the Pascal's law. All static limit quantities of $T^{\mu\nu}$ and N^μ are basically thermodynamical quantities like ϵ , P , n , which can be derived from the statistical mechanical description. For canonical ensemble or grand canonical ensemble, those macroscopic quantities can be derived from the single microscopic quantity-partition

function. Alternatively, one can define them via microscopic kinetic theory-based expression of the energy-momentum tensor and electron current

$$T_0^{\mu\nu} = N_s \int \frac{d^3\vec{p}}{(2\pi)^3} p^\mu v^\nu f_0 , \quad (5)$$

and

$$N_0^\mu = N_s \int \frac{d^3\vec{p}}{(2\pi)^3} v^\mu f_0 , \quad (6)$$

where $N_s = 2$ is spin degeneracy factor of electron and f_0 is its Fermi-Dirac distribution function $f_0 = 1/\{\exp(\beta(E - \mu)) + 1\}$. Where E = energy of fermions, μ = fermi energy i.e., the energy level up to the fermions fill or the maximum kinetic energy of fermions at absolute temperature.

The thermodynamics parameter β , which is $\beta = \frac{1}{k_B T}$ and k_B is Boltzmann constant and A is the fugacity of the system and which is, $A = \exp\left(\frac{\mu}{k_B T}\right)$.

Using the Eqs. (5) and (6), we will calculate the basic thermodynamical quantities - ϵ , P and n for different cases like G, NR, and UR, following energy and momentum relations or dispersion relations

$$\begin{aligned} E &= p v_g , \text{ for G case,} \\ &= p^2/(2m) , \text{ for NR case,} \\ &= p , \text{ for UR case,} \end{aligned} \quad (7)$$

respectively. For 3D case, we will consider $p^2 = p_x^2 + p_y^2 + p_z^2$ and $\int d^3p = \int 4\pi p^2 dp$, while for the 2D case, they will be considered as $p^2 = p_x^2 + p_y^2$ and $\int d^2p = \int 2\pi p dp$. We will elaborately address the 3D calculation for G case only, which will be followed for other cases - 3D NR, 3D UR, 2D G, 2D NR and 2D UR. So only final expressions of thermodynamical quantities for other cases will be written. They are addressed in the next two subsections for 3D and 2D systems, respectively.

A. Thermodynamic Quantities in 3D Space

From the equation (5), the energy density for the graphene system is

$$\epsilon_g^{3D} = T_0^{00} = N_s \int \frac{d^3p}{(2\pi)^3} (E) f_0. \quad (8)$$

After using the graphene dispersion relation $E = p v_g$, we get

$$\begin{aligned} \epsilon_g^{3D} &= \frac{N_s}{2\pi^2 v_g^3} \int_0^\infty \frac{E^3}{A^{-1} e^{\beta E} + 1} dE , \\ &= \frac{3N_s}{\pi^2 v_g^3} f_4(A) T^4 . \end{aligned} \quad (9)$$

Here, f_4 is Fermi integral function for $\nu = 4$, given in Eq. (1). From the Eq. (9), the total internal energy for V volume system can be written as

$$U_g^{3D} = \frac{3N_s V}{\pi^2 v_g^3} f_4(A) T^4 . \quad (10)$$

The total number of electrons in terms of the density of states can be written as

$$N = \int_0^\infty D(E) dE f_0 . \quad (11)$$

Here $D(E) dE$ is the number of energy states in energy range E to $E + dE$ and given in the appendix(A). Using it in the above equation (11), we get

$$N = N_s \frac{4\pi V}{(2\pi)^3 v_g^3} \int_0^\infty \frac{E^2}{A^{-1} e^{\beta E} + 1} dE .$$

After converting this integral into the Fermi integral function see in the appendix(B), we get the final expression of number density:

$$n_g^{3D} = \frac{N}{V} = \frac{N_s}{\pi^2 v_g^3} f_3(A) T^3. \quad (12)$$

One can get same expression of n_g^{3D} by starting from Eq. (6).

From the equations (9) and (12), we can write a relation between total internal energy $U = \epsilon V$ and total number $N = nV$ at finite volume V as

$$U_g^{3D} = 3NT \frac{f_4(A)}{f_3(A)}. \quad (13)$$

The electronic-specific heat for this system can be calculated by taking the derivative of total internal energy (U) with respect to temperature (T) at constant Fermi energy (μ) and constant V i.e.

$$[C_v] = \left. \frac{\partial U}{\partial T} \right|_{\mu, V}.$$

After applying this condition in appendix(C)(which is in 2D; similar to 3D) on Eq.(10), we get

$${}^3D_g [C_v]_e = \frac{[c_v]}{N} = 3k_B \left[4 \frac{f_4(A)}{f_3(A)} - \frac{\mu}{k_B T} \right]. \quad (14)$$

Now again from the equation (5), the pressure is

$$P_g^{3D} = T_0^{11} = N_s \int \frac{d^3 p}{(2\pi)^3} \left(\frac{E}{3} \right) f_0. \quad (15)$$

After solving this expression as similar to the energy density, we get the final more general expression of pressure for a 3D graphene system is

$$P_g^{3D} = \frac{N_s}{\pi^2 v_g^3} f_4(A) T^4. \quad (16)$$

Now, after doing the same type of calculation, if the Fermi velocity of electrons in graphene ' v'_g ' is replaced by the speed of light ' c ', then the system becomes ultra-relativistic (UR). While $[C_v]_e$ is independent of velocity, the specific heat will be the same for G and UR cases.

And also, for a 3D NR system, if a similar calculation is done, then the more general expressions in terms of the Fermi-Dirac function/Fermi-integral function of energy density, electronic specific heat, number density, and pressure become like this:

$$\epsilon_{NR}^{3D} = \frac{3N_s}{2} \left(\frac{m}{2\pi} \right)^{\frac{3}{2}} f_{\frac{5}{2}}(A) T^{\frac{5}{2}}, \quad (17)$$

$${}^3D_{NR} [C_v]_e = \frac{[c_v]}{N} = \frac{3}{2} k_B \left[\frac{5}{2} \frac{f_{\frac{5}{2}}(A)}{f_{\frac{3}{2}}(A)} - \frac{\mu}{k_B T} \right], \quad (18)$$

$$n_{NR}^{3D} = N_s \left(\frac{m}{2\pi} \right)^{\frac{3}{2}} f_{\frac{3}{2}}(A) T^{\frac{3}{2}}, \quad (19)$$

$$P_{NR}^{3D} = N_s \left(\frac{m}{2\pi} \right)^{\frac{3}{2}} f_{\frac{5}{2}}(A) T^{\frac{5}{2}}. \quad (20)$$

TABLE I. 3D systems at $\mu \rightarrow 0$ limits: Thermodynamical quantities - energy density ϵ , pressure P , number density n for NR, G and UR cases.

	NR	G	UR
ϵ	$1.94 \left(\frac{m}{2\pi}\right)^{3/2} \zeta_{5/2} T^{5/2} = (6.03 \times 10^7) T^{5/2}$	$\frac{6}{\pi^2} \frac{7}{8} \zeta_4 T^4 = (0.2665 \times 10^7) T^4$	$\frac{6}{\pi^2} \frac{7}{8} \zeta_4 T^4 = 0.5756 T^4$
P	$1.29 \left(\frac{m}{2\pi}\right)^{3/2} \zeta_{5/2} T^{5/2} = (4.02 \times 10^7) T^{5/2}$	$\frac{2}{\pi^2} \frac{7}{8} \zeta_4 T^4 = (0.0888 \times 10^7) T^4$	$\frac{2}{\pi^2} \frac{7}{8} \zeta_4 T^4 = 0.1919 T^4$
n	$0.59 \left(\frac{m}{2\pi}\right)^{3/2} \zeta_{3/2} T^{3/2} = (3.55 \times 10^7) T^{3/2}$	$\frac{2}{\pi^2} \frac{3}{4} \zeta_3 T^3 = (0.0846 \times 10^7) T^3$	$\frac{2}{\pi^2} \frac{3}{4} \zeta_3 T^3 = 0.1827 T^3$

TABLE II. 3D systems at $T \rightarrow 0$ limits: Thermodynamical quantities - energy density ϵ , pressure P , number density n for NR, G and UR cases.

	NR	G	UR
ϵ	$\frac{2\sqrt{2}}{5\pi^2} m^{3/2} \mu^{5/2} = (2.09 \times 10^7) \mu^{5/2}$	$\frac{1}{4\pi^2 v_g^3} \mu^4 = (0.0117 \times 10^7) \mu^4$	$\frac{1}{4\pi^2} \mu^4 = 0.025 \mu^4$
P	$\frac{4\sqrt{2}}{15\pi^2} m^{3/2} \mu^{5/2} = (1.39 \times 10^7) \mu^{5/2}$	$\frac{1}{12\pi^2 v_g^3} \mu^4 = (0.0039 \times 10^7) \mu^4$	$\frac{1}{12\pi^2} \mu^4 = 0.008 \mu^4$
n	$\frac{2\sqrt{2}}{3\pi^2} m^{3/2} \mu^{3/2} = (3.49 \times 10^7) \mu^{3/2}$	$\frac{1}{3\pi^2 v_g^3} \mu^3 = (0.0156 \times 10^7) \mu^3$	$\frac{1}{3\pi^2} \mu^3 = 0.034 \mu^3$

B. Thermodynamic Quantities in 2D Space

In the 3D graphene case if term $\frac{d^3 p}{(2\pi)^3}$ changes into $\frac{d^2 p}{(2\pi)^2}$ then the above similar way of calculation we get all the expressions in the more general form of energy density, electronic specific heat, number density and pressure for 2D graphene system. After doing the calculation, we get

$$\epsilon_g^{2D} = \frac{U}{V} = \frac{N_s}{\pi v_g^2} f_3(A) T^3, \quad (21)$$

$${}^{2D} [C_v]_e = \frac{[c_v]}{N} = 2k_B \left[3 \frac{f_3(A)}{f_2(A)} - \frac{\mu}{k_B T} \right], \quad (22)$$

$$n_g^{2D} = \frac{N}{V} = \frac{N_s}{2\pi v_g^2} f_2(A) T^2, \quad (23)$$

$$P_g^{2D} = \frac{N_s}{2\pi v_g^2} f_3(A) T^3. \quad (24)$$

If, in the above results, the ' v'_g ' is replaced by 'c', all results become a 2D UR system. And after doing the same calculation for a 2D NR system, then we get the energy density, electronic specific heat, number density, and pressure which are given as

$$\epsilon_{NR}^{2D} = \frac{N_s}{2} \left(\frac{m}{\pi}\right) f_2(A) T^2, \quad (25)$$

$${}^{2D}_{NR} [C_v]_e = \frac{[c_v]}{N} = k_B \left[2 \frac{f_2(A)}{f_1(A)} - \frac{\mu}{k_B T} \right], \quad (26)$$

$$n_{NR}^{2D} = \frac{N_s}{2} \left(\frac{m}{\pi}\right) f_1(A) T, \quad (27)$$

$$P_{NR}^{2D} = \frac{N_s}{2} \left(\frac{m}{\pi}\right) f_2(A) T^2. \quad (28)$$

III. RESULTS

In the Formalism part, we have obtained the general expressions of different thermodynamical quantities like energy density, pressure, number density, specific heat, etc. for electron fluid inside graphene, where fluid particle - electrons follow the dispersion relation $E = p v_g$. In parallel, we also have addressed the corresponding expressions for

TABLE III. 2D systems at $\mu \rightarrow 0$ limits: Thermodynamical quantities - energy density ϵ , pressure P , number density n for NR, G and UR cases.

	NR	G	UR
ϵ	$\frac{1}{2} \left(\frac{m}{\pi}\right) \zeta_2 T^2 = (1.34 \times 10^5) T^2$	$\frac{2}{\pi} \frac{3}{v_g^2} \zeta_3 T^3 = (0.1594 \times 10^5) T^3$	$\frac{2}{\pi} \frac{3}{4} \zeta_3 T^3 = 0.5739 T^3$
P	$\frac{1}{2} \left(\frac{m}{\pi}\right) \zeta_2 T^2 = (1.34 \times 10^5) T^2$	$\frac{1}{\pi} \frac{3}{v_g^2} \zeta_3 T^3 = (0.7971 \times 10^4) T^3$	$\frac{1}{\pi} \frac{3}{4} \zeta_3 T^3 = 0.2870 T^3$
n	undefined	$\frac{1}{\pi} \frac{1}{v_g^2} \zeta_2 T^2 = (0.7184 \times 10^4) T^2$	$\frac{1}{\pi} \frac{1}{2} \zeta_2 T^2 = 0.2586 T^2$

TABLE IV. 2D systems at $T \rightarrow 0$ limits: Thermodynamical quantities - energy density ϵ , pressure P , number density n for NR, G and UR cases.

	NR	G	UR
ϵ	$\frac{m}{2\pi} \mu^2 = (8.13 \times 10^4) \mu^2$	$\frac{1}{3\pi} \frac{1}{v_g^2} \mu^3 = (2.9473 \times 10^3) \mu^3$	$\frac{1}{3\pi} \mu^3 = 0.106 \mu^3$
P	$\frac{m}{2\pi} \mu^2 = (8.13 \times 10^4) \mu^2$	$\frac{1}{3\pi} \frac{1}{v_g^2} \mu^3 = (2.9473 \times 10^3) \mu^3$	$\frac{1}{3\pi} \mu^3 = 0.106 \mu^3$
n	$\frac{m}{\pi} \mu = (1.63 \times 10^5) \mu$	$\frac{1}{2\pi} \frac{1}{v_g^2} \mu^2 = (4.4209 \times 10^3) \mu^2$	$\frac{1}{2\pi} \mu^2 = 0.159 \mu^2$

electrons following NR dispersion relation $E = p^2/(2m)$ and UR dispersion relation $E = pc$ for numerical comparison, which will be presented here in this results section. Through this comparative analysis, our aim is to highlight that graphene thermodynamics is neither non-relativistic nor ultra-relativistic thermodynamics. Just like they are different in microscopic dispersion relations, similarly, they are different in macroscopic thermodynamics also.

Before drawing the general expressions of three cases - G, NR, and UR for 2D and 3D systems, which are expressed in terms of Fermi integral form in the formalism part, let us first provide a tabulated description of their simple expressions in two extreme limits - (1) $\mu \rightarrow 0$ and (2) $T \rightarrow 0$. Tables (I) and (II) cover thermodynamics in $\mu \rightarrow 0$ and $T \rightarrow 0$ limits respectively for 3D systems. Next, tables (III) and (IV) cover the same for 2D systems.

Let us see the table (I), demonstrating $\mu \rightarrow 0$ limits of 3D system thermodynamics for NR, G, and UR cases. The reader may find the beauty of two limits - the power of T -dependence for thermodynamical quantities in $\mu \rightarrow 0$ limit remains the same in $T \rightarrow 0$ limit, the only powers of T are converted to the powers of μ . The constants, attached with the T or μ -dependent terms are different. By taking an example of energy density for 3D UR case, we can see that constants are changing from $\epsilon/T^4 = 0.57$ to $\epsilon/\mu^4 = 0.02$ due to transition from Stefan Boltzmann (SB) limit ($\mu \rightarrow 0$) to degenerate gas limit ($T \rightarrow 0$). If we take other examples also, then the reader can notice a common fact for any thermodynamical quantities of any cases that the constants are transiting from lower to higher values during the transition from degenerate gas limit to SB limit. This may be connected with an interesting fact if we interpret it as follows. Thermodynamics is basically many body outcomes and a summation of one body quantity. After summing one body's microscopic energy scale, we get thermodynamics in terms of macroscopic energy scales μ and T with some powers. So we may assume that the constants of ϵ/T^4 , P/T^4 , n/T^3 in SB limit and the constants of ϵ/μ^4 , P/μ^4 , n/μ^3 in degenerate gas limit are basically some outcomes connected with a statistical summation. Its values are growing, which may mean that its statistical summations are growing and the thermodynamic system is going towards more thermodynamics, where the local thermalization concept can be applied. Or in other words, the thermodynamical system approaches the hydrodynamical system. As an example, when we take nuclear or quark matter in the SB limits, expected in high energy heavy ion collisions, we get their hydrodynamical system.

According to the table (II), we can see that G and UR follow similar μ -dependence: $\epsilon \propto P \propto \mu^4$, $n \propto \mu^3$ but in order of magnitude, $G \gg UR$ because $v_g^3 \ll c^3$ (our expressions in the table are in natural unit, where $c = 1$ is considered for UR case). Unlike the μ -dependence of G or UR case, NR follows $\epsilon \propto P \propto \mu^{5/2}$, $n \propto \mu^{3/2}$ but in order of magnitude, it is larger than G. In terms of order of magnitude, we can conclude a gross ranking: $NR > G \gg UR$, which will be more clear in the graphical representation later.

Next, In Tables (III), (IV), 2D thermodynamical expressions in SB limits and degenerate for NR, G, and UR cases are addressed. We notice the transition from $\epsilon \propto P \propto nT \propto T^4$ to $\epsilon \propto P \propto nT \propto T^3$ for G/UR case and from $\epsilon \propto P \propto nT \propto T^{5/2}$ to $\epsilon \propto P \propto nT \propto T^2$ for NR case due to 3D \rightarrow 2D transition. A similar change in the power of chemical potential is noticed for degenerate results. The except thing is that in the SB limit, the number density of 2D NR system is found to be undefined. In general, any thermodynamical quantity depends on $f_n T^n$, where n (not to be confused with number density) is an index of the Fermi integral function and power of T . Now in the SB limit or $\mu \rightarrow 0$ limit, we get $f_n T^n \rightarrow (1 - \frac{1}{2^{n-1}}) \zeta_n T^n$, which will be undefined for $n = 1$ as $(1 - \frac{1}{2^{1-1}})$ is zero and $\zeta_1 = \infty$. Interestingly, we don't find any realistic example of NR system with zero Fermi energy in 2D and 3D cases. For metal,

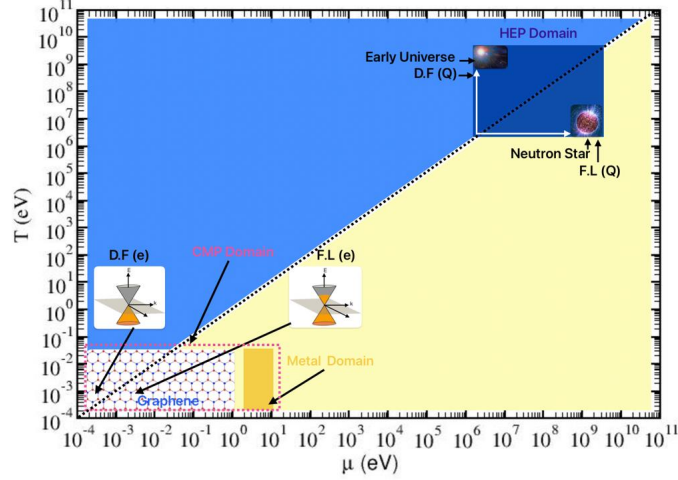


FIG. 1. The Condensed Matter Physics (CMP) and high energy physics (HEP) locations and their Dirac Fluid (DF) and Fermi Liquid (FL) domains in T - μ plane.

Fermi energy or chemical potential of electron locate within $\mu = 2$ -10 eV range.

Let us go to a brief discussion on Quark Gluon Plasma (QGP), which is a more realistic UR case example than a hypothetical case - UR electron fluid. Just after a few micro-second from the big bang, a hot quark-gluon plasma (QGP) state around temperature $T = 400$ MeV or $T = 700$ MeV, and zero quark chemical potential ($\mu = 0$) is expected in the early universe scenario. The quark average momenta become so large because of high temperature that we can ignore its mass term, and it can be considered a UR case. Photon gas or black body radiation example is famous for UR case, where internal energy density or Intensity (they have connecting relation) follows T^4 law, popularly known as Stefan-Boltzmann (SB) law. QGP thermodynamics at high temperatures reaches that SB limits. Energy density, pressure, number density for 3D UR case, given in Table (I), can be used for the quark system by replacing its relevant degeneracy factors. For two-flavor quark has a degeneracy factor of 24. On the other hand, when one goes to $T \rightarrow 0$ limit, UR case of Table (II) can be applied for the thermodynamics of the degenerate quark system, may be expected in the core of neutron star. In this degenerate gas limit, degeneracy factor 12 which has to be considered as anti-particle probability will be highly suppressed.

We have to understand the difference between the temperature range of QGP and the graphene system. QGP temperature is a few hundred mega electron Volt (MeV) and equivalent to 10^{12} $^{\circ}$ K, which is too much larger than the temperature range of the graphene system. Typically, 1 – 25 milli electron Volt (*meV*) or equivalently 15 – 300 $^{\circ}$ K is the graphene system temperature range. These two domains are nicely addressed in Fig. (1), where T vs. μ plots in the log scale have covered a broad band of T and μ range. The condensed matter physics (CMP) domain specifies the temperature range of approximately 1 – 25 meV and the chemical potential range of approximately 0 – 10 eV.

The range of chemical potential μ from 2 – 10 eV is associated with the metal Fermi energy by marking it as yellow. Unlike metals, the Fermi energy in a graphene system can be modified or tuned through various doping methods, and its $\mu/T \ll 1$ and $\mu/T \gg 1$ domains are called Dirac fluid (DF) or Dirac liquid (DL) and Fermi liquid (FL) domains, respectively, marked by arrows in Fig. (1). We may call early universe QGP as DF domain of quark and quark matter, anticipated in the core of neutron star as FL domain of quark. A rectangular domain within $T = 1 - 400$ MeV and $\mu = 0 - 1000$ MeV is marked as high energy physics (HEP) domain for quark. The reader can easily notice the gap between CMP and HEP domains.

We understand the scale gap in T - μ plane between UR case of the quark system and the G case of electron system. So, to see in the same T - μ scale, we must consider a hypothetical electron ultra-relativistic fluid (URF) to make an equal footing comparison with electron graphene fluid (GF). We can call ϵ , P , n of UR case in Tables (I) and (III) as ϵ_{SB} , P_{SB} , n_{SB} . Next putting $v_g = c = 1$ in ϵ , P , n of Eqs. (10), (12), (16), we get

$$\begin{aligned}
 U_{UR}^{3D} &= \frac{3N_s V}{\pi^2} f_4(A) T^4, \\
 n_{UR}^{3D} &= \frac{N}{V} = \frac{N_s}{\pi^2} f_3(A) T^3, \\
 P_{UR}^{3D} &= \frac{N_s}{\pi^2} f_4(A) T^4.
 \end{aligned} \tag{29}$$

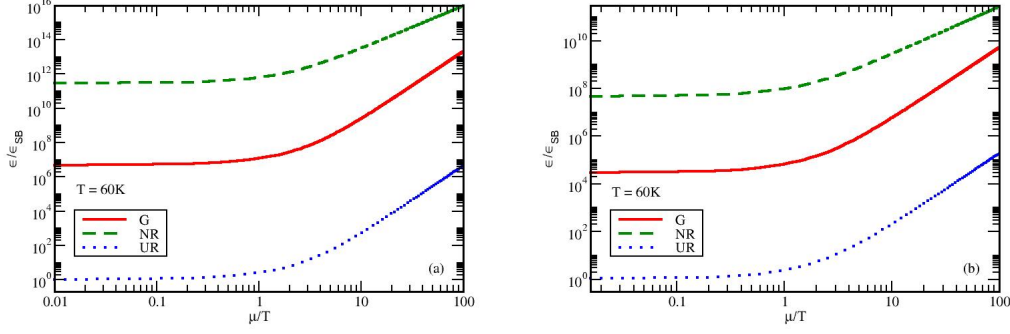


FIG. 2. The energy density in different domains to ϵ_{SB} with μ/T for (a) 3D case and (b) for 2D case.

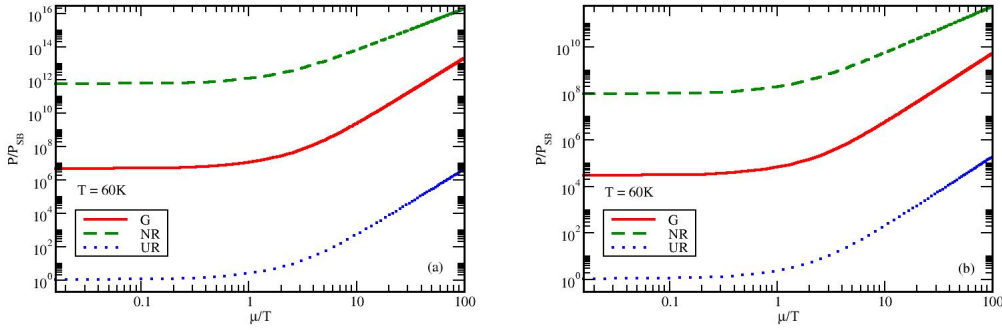


FIG. 3. The Pressure in different domains to P_{SB} with μ/T for (a) 3D case and (b) 2D case.

Normalizing Eqs. (29) by their SB limits, we have sketched them by the blue dotted lines in the left panel of Figs. (2), (3), (4) which become one in the domain $\mu/T \ll 1$, as expected. Interestingly, we noticed that the main μ/T dependence in thermodynamical quantities is coming beyond the $\mu/T = 1$. It is Fermi integral functions, which are the main source of μ/T dependence. Next, the red solid lines in the left panel of Figs. (2), (3), (4) represent the graphene thermodynamics, where Fermi velocity $v_g = 0.006$ is considered. We have considered in-between constant values $v_g = 0.006$ from the Fermi velocity range $v_g = 1 - 3 \times 10^6$ m/s or $v_g = 0.003 - 0.01$ (in natural unit) in graphene system [35]. The noticeable point is that μ/T dependence of UR and G thermodynamics are the same but $G \gg UR$ due to the $1/v_g^3 \approx 5 \times 10^6$ term. Next, we use Eqs. (17), (19), (20) to draw NR thermodynamical quantities (green dashed lines). In terms of order of magnitude, we get ranking $UR \ll G \ll NR$.

A similar trend can notice for 2D cases with similar ranking $URF \ll GF \ll NRF$. Only for the transition from 3D to 2D, their orders of magnitude are shifted toward lower values.

There is a famous equi-partition law, which states that energy density by number density ϵ/n will be equal to the number of degrees of freedom times $\frac{1}{2}k_B T$. If we define degrees of freedom as D , then $\frac{\epsilon}{n} = \frac{D}{2}T$ (in natural unit $k_B = 1$). Therefore, for 3D system having three degrees of freedom, $\frac{\epsilon}{nT} = \frac{3}{2} = 1.5$ and for 2D system having two degrees of freedom, $\frac{\epsilon}{nT} = \frac{2}{2} = 1$. These two horizontal dotted lines at 1.5 and 1 are drawn in the left and right panels of Fig. (5). This is true for ideal classical gas, whose constituent particles follow Maxwell Boltzmann (MB) statistics and NR dispersion relation, but for ideal quantum electron gas, whose constituent particles follow FD statistics, the equi-partition law becomes little modified. The $\frac{\epsilon}{nT}$ does not remain constant; it will change with μ/T as shown by the green dash line for NR electron gas. Interestingly the major changes or diverging trend is noticed beyond $\mu/T = 1$ or FL domain, while in DF domain, it is almost saturated towards the value 1.72, which is slightly greater than 1.5. This small deviation from 1.5 to 1.72, shown in the left panel of Fig. (5), is basically due to the quantum statistical effect. Same deviation from 1 to 1.2 [36] can be seen in the right panel of Fig. (5) for 2D NR system.

Next, when we go for UR and G cases, interestingly, both follow the same equi-partition law as demonstrated by the red line of Fig. (5). The reason for merging between UR and G in $\frac{\epsilon}{nT}$ is as follows. The main difference

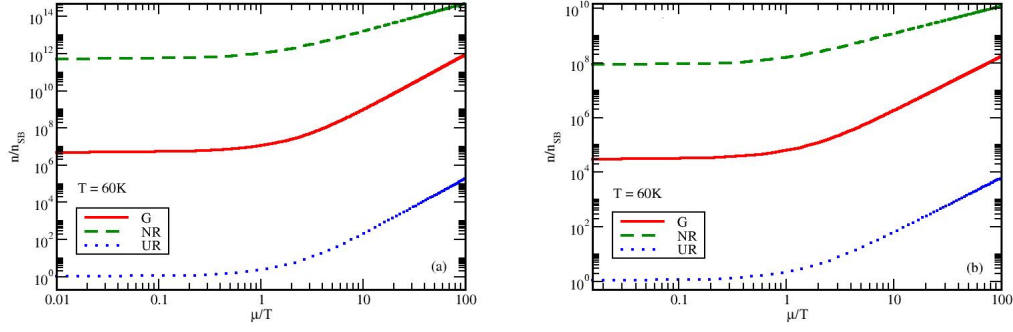


FIG. 4. The number density in different domains to n_{SB} with μ/T (a) in the 3D case and (b) in the 2D case.

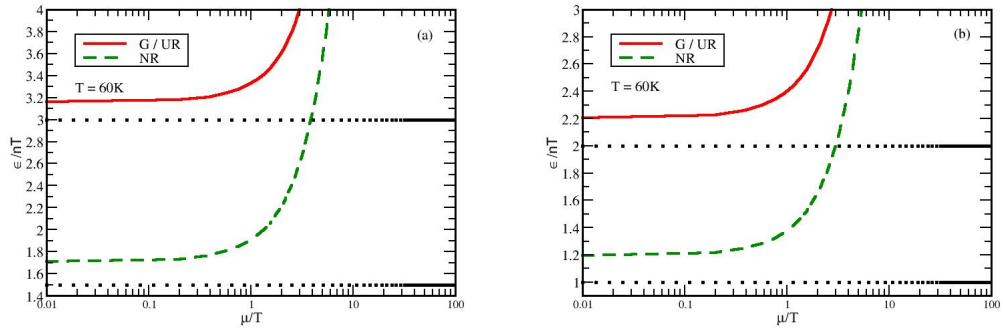


FIG. 5. The ratio of the energy density and number density for (a) 3D and (b) 2D systems.

between UR and G thermodynamical quantities is due to the role of c and v_g in their respective expressions. During calculating ratio $\frac{\epsilon}{nT}$, they are canceled, so their ratio becomes exactly the same. Here also, for ideal classical gas, one can formulate equi-partition law for UR gas as follows. Energy density by number density ϵ/n will be equal to the number of degrees of freedom times T instead of $\frac{1}{2}T$. If we define degrees of freedom as D , then $\frac{\epsilon}{n} = DT$, which means $\frac{\epsilon}{nT} = 3$ for 3D system and $\frac{\epsilon}{nT} = 2$ for 2D system as drawn in left and right panels of Fig. (5). Due to quantum statistical effect, $\frac{\epsilon}{nT}$ UR or G gas will shift from 3 to 3.15 for 3D case and from 2 to 2.21 for 2D case. We can define the quantum statistical factor as $Q_{G/UR}$ and Q_{NR} for G/UR and NR system at $\mu = 0$ to formulate equi-partition

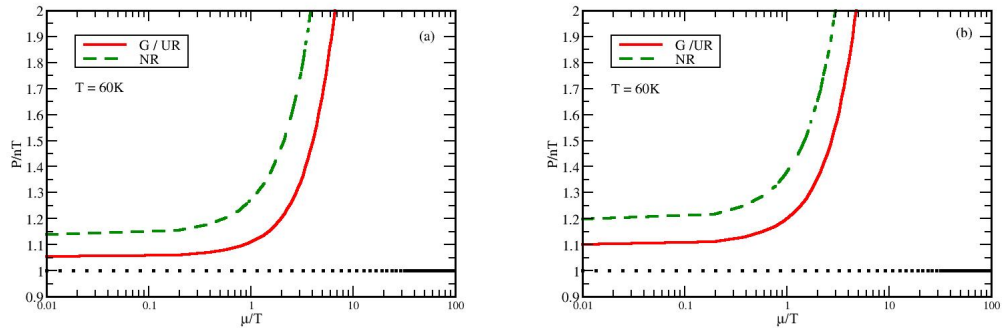


FIG. 6. The ratio of the pressure and number density for (a) 3D and (b) 2D systems.

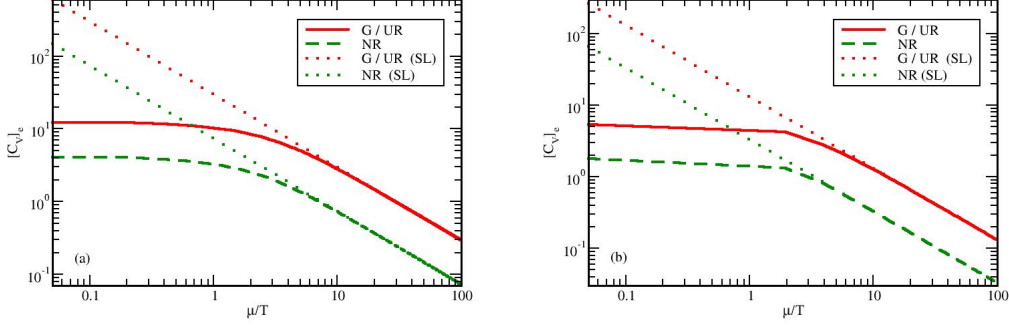


FIG. 7. The Comparison of SL and finite cases of specific heat capacity for (a) 3D case and (b) 2D case.

law:

$$\begin{aligned} \frac{\epsilon}{nT} &= D \times Q_{G/UR} \text{ for G/UR case ,} \\ &= \frac{D}{2} \times Q_{NR} \text{ for NR case ,} \end{aligned} \quad (30)$$

with

$$\begin{aligned} Q_{G/UR} &= \frac{(1 - 1/2^3) \zeta_4}{1 - 1/2^2 \zeta_3} \text{ for 3D system ,} \\ &= \frac{(1 - 1/2^2) \zeta_3}{1 - 1/2 \zeta_2} \text{ for 2D system ,} \\ Q_{NR} &= \frac{(1 - 1/2^{3/2}) \zeta_{5/2}}{1 - 1/2^{1/2} \zeta_{3/2}} \text{ for 3D system ,} \\ &= 1.2 \text{ for 2D system .} \end{aligned} \quad (31)$$

These quantum statistical factors almost become independent of μ/T in DF domain, and we may safely consider the values of $\mu = 0$, given in Eq. (31). However, in the FL domain, one should consider quantum statistical factors in terms of Fermi integral functions as

$$\begin{aligned} Q_{G/UR} &= \frac{f_4}{f_3} \text{ for 3D system ,} \\ &= \frac{f_3}{f_2} \text{ for 2D system ,} \\ Q_{NR} &= \frac{f_{5/2}}{f_{3/2}} \text{ for 3D system ,} \\ &= \frac{f_2}{f_1} \text{ for 2D system .} \end{aligned} \quad (32)$$

After exploring the equi-partition law, let us come to the equation of state (EoS), relating P and n . For ideal classical gas, we know that though $\frac{\epsilon}{nT}$ depends on dispersion relations $E \propto p$ or $E \propto p^2$ as well as dimension D , but $\frac{P}{nT}$ remains independent of those. Ideal gas EoS always becomes $\frac{P}{nT} = 1$ for any cases 3D/2D or NR/G/UR, which are shown by dotted horizontal lines in Fig. (6)(a) and (b). Now actual 3D, 2D electron NR, G and UR gas, following FD statistics, will have EoS $\frac{P}{nT} > 1$ due to same quantum statistical factors, described by (31) for DF and Eq. (32) for FL.

Finally, we constructed the directly measurable thermal quantity, the electronic specific heat capacity of graphene, and NR in Fig. (7) in terms of μ/T . In Fig. (7), T is fixed at $T = 60^0$ K and μ is varied. Here, the green lines are represented by NR, and the red lines are for G or UR cases. Since $\frac{\epsilon}{n} = \frac{U}{N}$ for both G and UR are the same, their temperature derivative, which is basically specific heat per electron, also becomes the same. In $\mu/T \gg 1$ or FL

domain, Sommerfeld's limits (SL) can be applied to Eqs. (14), (18), (22), (26) for 3D-G, 3D-NR, 2D-G and 2D-NR systems and their expressions will be converted into very simple forms:

$$\begin{aligned}
{}^3D_g[C_v]_e &= 3\pi^2 \frac{T}{\mu}, \\
{}^3D_{NR}[C_v]_e &= \frac{3\pi^2}{4} \frac{T}{\mu}, \\
{}^2D_g[C_v]_e &= \frac{4\pi^2}{3} \frac{T}{\mu}, \\
{}^2D_{NR}[C_v]_e &= \frac{\pi^2}{3} \frac{T}{\mu}.
\end{aligned} \tag{33}$$

They are plotted by dotted lines in Fig. (7), whose trends indicate the standard $C_v \propto \frac{T}{\mu}$ relation as expected for metal for the low-temperature domain. For metal, Fermi energy or μ remains almost constant with T ; therefore, the standard practice is to consider the metal electron-specific heat as proportional to T . So, our NR case SL expression may be used as metal electronic specific heat contribution. However, the proportional constant of $C_v \propto T$ will be a bit of different from standard Solid state physics book [37], where number density and volume is kept constant but we have used the definition, where μ and volume are kept constant. Reader may comprehend the constant number density and volume definition of specific heat as a solid state-based definition, whereas the constant μ and volume definition of specific heat may be considered as a fluid-based definition. We know that (almost) in-compressible solid-based formalism for electrons in the metal, thermodynamical quantities like P , V , N never be a matter of interest to calculate as they always remain constant but its U and C_v are normally calculated by using quantum statistical formalism in the $\mu/T \gg 1$ limit, which is basically free electron theory, practiced in solid state physics book [37]. For the metal case, we can't decrease Fermi energy μ below $\mu/T = 1$ as their approximate range is $\mu = 2-10$ eV, which almost remains constant with T . It was graphene, where carrier density n can be tuned by changing T and μ , So one can access the range lower than $\mu/T = 1$, even can reach DF domain - $\mu/T \ll 1$. In this DF region, SL $C_v \propto T$ is not at all valid, one should use the general expression, given in Eq. (22). Understanding the transition from solid-based (SL expressions) to fluid-based (general expressions) formulas of specific heat may be very important to realize Wiedemann-Franz (WF) Law violation in DF domain, observed in Refs. [26]. Being proportional with specific heat, modification of thermal conductivity in DF domain is possible for which the ratio between thermal and electrical conductivity may not follow WF law. This is our immediate future plan of work where we plan a systematic transformation from solid-based to fluid-based calculations of specific heat, thermal conductivity as well as electrical conductivity.

IV. SUMMARY

In summary, the present work is focused on thermodynamic aspects of the graphene system after getting inspiration from the recent discovery of electron hydrodynamics in the graphene system. This experimental discovery has opened a new scope of analytic calculations in condensed matter physics, which was traditionally well cultivated in science and engineering as non-relativistic hydrodynamics and in high energy nuclear and astro physics as relativistic hydrodynamics. An interesting fact about electrons in graphene is that it follows neither non-relativistic nor relativistic hydrodynamics. Present work has highlighted that fact by concentrating on the ideal part of the energy-momentum tensor and current of electrons in graphene, whose static limit quantities are basically thermodynamical quantities like pressure, energy density, etc. The present article has gone through systematic microscopic calculations of that graphene thermodynamics and compared them with corresponding estimations for non-relativistic and ultra-relativistic cases. Firstly, at low temperatures (around 60⁰ K), Dirac fluid (DF) and Fermi liquid (FL) domains are respectively marked for low and high Fermi energy, and then electron thermodynamics for graphene and other cases are sketched to see their estimations in those two domain. From the final expressions and graphs of those thermodynamics for 3 dimensions (3D) and 2 dimensions (2D) graphene (G), non-relativistic (NR) and ultra-relativistic (UR) cases, we can highlight our findings in a few bullet points as:

- We find the ranking $UR \ll G \ll NR$ and $2D \ll 3D$ in terms of order of magnitude of thermodynamical quantities - pressure, energy density and number density.
- Interestingly, G and UR both follow the same equation state $\frac{P}{nT} = Q$ and equi-partition law $\frac{\epsilon}{nT} = D Q$, where D is the dimension of systems and Q is its corresponding quantum statistical factors in terms of Fermi integral function for FL domain and Riemann-Zeta function for DF domain. On the other hand, NR case follows equation

state $\frac{P}{nT} = Q$ and equi-partition law $\frac{\epsilon}{nT} = \frac{D}{2} Q$, where Q is its corresponding quantum statistical factors for NR case.

- We have interpreted the general expression of specific heat as a fluid-based expression, applicable for DF domain, while its Sommerfeld limit gives a solid-based expression, applicable for the FL domain. This interpretation may be connected to the experimentally observed Wiedemann-Franz Law violation in DF domain of the graphene system.

We have considered mili-electron Volt order temperature and electron Volt order Fermi energy for all cases, including the UR case. However, as a realistic example, quark matter at few hundred Mega electron Volt temperature and thousands Mega electron Volt Fermi energy or chemical potential is a good example. Similar to FL to DF transition in the condensed matter physics domain, an equivalent transition for quark matter in the high energy physics domain is also discussed.

ACKNOWLEDGMENTS

This work was partly (TZW and CWA) supported by the Doctoral Fellowship in India (DIA) program of the Ministry of Education, Government of India. The authors thank the other members of eHD club - Sesha P. Vempati, Ashutosh Dwibedi, Narayan Prasad, Bharat Kukkar, and Subhalaxmi Das Nayak.

Appendix A: Density of States

The density of states is nothing but the total number of energy states per unit energy interval. If the total number of energy states in energy range E to $E + dE$ are $D(E) dE$ then the density of states will be

$$g(E) = \frac{D(E) dE}{dE} . \quad (\text{A1})$$

Case:1. for 3D Graphene,

$$D(E) dE = N_s \frac{4\pi V}{h^3 v_g^3} E^2 dE . \quad (\text{A2})$$

Case:2. for 3D Non-Relativistic,

$$D(E) dE = N_s 2\pi V \left(\frac{2m}{h^2} \right)^{\frac{3}{2}} \sqrt{E} dE . \quad (\text{A3})$$

Case:3. for 2D Graphene,

$$D(E) dE = N_s \frac{2\pi S}{h^2 v_g^2} E dE . \quad (\text{A4})$$

Case:4. for 2D Non-Relativistic,

$$D(E) dE = N_s \frac{2\pi S}{h^2} m dE . \quad (\text{A5})$$

In the above expressions, V and S represent the volume and area in position space, respectively.

Appendix B: Fermi-Dirac Function

The Fermi-Dirac integral Function

$$f_\nu(A) = \frac{1}{\Gamma(\nu)} \int_0^\infty \frac{x^{\nu-1}}{A^{-1}e^x + 1} dx . \quad (\text{B1})$$

Case:1

When $\mu \rightarrow 0$ (i.e., $\mu/T \ll 1$), then the Fermi-Dirac function can be written in a series form which is

$$f_\nu(A) = \left(1 - \frac{1}{2^{n-1}}\right) \zeta_n . \quad (\text{B2})$$

Case:2

When the temperature is very small, and the Fermi energy has some finite values (i.e., $\mu/T \gg 1$), then the Fermi-Dirac function can be written according to Sommerfeld's lemma, which gives the expression of the function as

$$f_\nu(A) = \frac{\alpha^\nu}{\Gamma(\nu+1)} \left[1 + \nu(\nu-1) \frac{\pi^2}{6} \frac{1}{\alpha^2} + \nu(\nu-1)(\nu-2)(\nu-3) \frac{7\pi^4}{360} \frac{1}{\alpha^4} + \dots \right] . \quad (\text{B3})$$

Where α is given by, $\alpha = \ln A = \frac{\mu}{k_B T}$.

- The derivative of Fermi function with respect to Fermi energy

$$\left(\frac{\partial f_\nu(A)}{\partial \mu} \right) = \beta f_{\nu-1}(A) . \quad (\text{B4})$$

- The derivative of Fermi function with respect to temperature

$$\left(\frac{\partial f_\nu(A)}{\partial T} \right) = \frac{1}{A} f_{\nu-1}(A) \frac{\partial A}{\partial T} . \quad (\text{B5})$$

And the one identity for the function can be written as

$$\frac{1}{A} \frac{\partial A}{\partial T} = -\mu \beta^2 k_B = -\frac{\mu}{k_B T^2} . \quad (\text{B6})$$

Appendix C: Electronic Specific Heat Capacity

For 2D system graphene, which follows the dispersion relation in Eq. (7), considering this type of system with the help of the density of state method, we can calculate the number density, total internal energy, and the electronic-specific heat.

So, the number of energy states in the energy range E to $E + dE$ is written as

$$D(E) dE = N_s \frac{S}{(2\pi)^2} \frac{2\pi}{v_g^2} E dE , \quad (\text{C1})$$

where S is the surface area of the electron fermionic system. Now, the total number of particles at any value of temperature can be calculated as

$$N = \int_0^\infty D(E) dE f_0(E) . \quad (\text{C2})$$

After plugging the value of $D(E) dE$ in the above equation, we get

$$n = \frac{N}{S} = \frac{N_s}{2\pi v_g^2} \int_0^\infty \frac{E}{A^{-1} e^{\beta E} + 1} dE . \quad (\text{C3})$$

For 2D, n is the number of particles per unit area, so S is surface area. After solving this integration, we get the final more general expression of number density which is given by

$$N = N_s \frac{2\pi S \Gamma(2)}{h^2 v_g^2 \beta^2} f_2(A) , \quad (C4)$$

$$n = N_s \frac{2\pi}{h^2 v_g^2} f_2(A) T^2 . \quad (C5)$$

Now, the total internal energy of a system can be calculated as

$$U = \int_0^\infty D(E) dE E f_0(E) . \quad (C6)$$

After plugging the value of $D(E) dE$ in the above equation and solving the integration, we get the final more general expression of total internal energy which is given by

$$U = N_s \frac{2\pi S \Gamma(3)}{h^2 v_g^2 \beta^3} f_3(A) . \quad (C7)$$

Now, from equation (C4) and (C7), we get

$$U = 2NT \frac{f_3(A)}{f_2(A)} . \quad (C8)$$

Now we can calculate the specific heat capacity with the help of total internal energy expression by taking the derivative of U with respect to temperature for a constant chemical potential μ and area S in 2D. So, specific heat capacity is

$$C_v = \left. \frac{\partial U}{\partial T} \right|_{\mu, S} . \quad (C9)$$

From the Eq.(C7), total internal energy is

$${}^{2D}_g U = N_s \frac{2\pi S \Gamma(3)}{h^2 v_g^2 \beta^3} f_3(A) , \quad (C10)$$

$$= N_s \frac{2\pi S}{h^2 v_g^2} \Gamma(3) k_B^3 T^3 f_3(A) , \quad (C11)$$

$$= \gamma T^3 f_3(A) , \quad (C12)$$

where

$$\gamma = N_s \frac{2\pi S}{h^2 v_g^2} \Gamma(3) k_B^3 .$$

Now, after taking the derivative of just the above equation with respect to T at constant Fermi energy and volume, we get

$$C_v = \gamma \left[3T^2 f_3(A) + T^3 f_2(A) \frac{1}{A} \frac{\partial A}{\partial T} \right] , \quad (C13)$$

$$= \gamma T^2 f_2(A) \left[3 \frac{f_3(A)}{f_2(A)} + T \frac{1}{A} \frac{\partial A}{\partial T} \right] . \quad (C14)$$

After using the identity (B6), and also from the Eq.(C4), the relation between N and γ can be written as

$$\gamma T^2 f_2(A) = 2Nk_B ,$$

and now Eq.(C14) becomes

$$C_v = 2Nk_B \left[3 \frac{f_3(A)}{f_2(A)} - \frac{\mu}{k_B T} \right].$$

Now, the final expression of electronic-specific heat per particle can be written in a more general form as

$${}^2D_g[C_v]_e = \frac{c_v}{N} = 2k_B \left[3 \frac{f_3(A)}{f_2(A)} - \frac{\mu}{k_B T} \right]. \quad (\text{C15})$$

-
- [1] D. J. Acheson, *Elementary fluid dynamics* (1991).
- [2] D. Tong, *Kinetic theory*, Graduate Course, University of Cambridge, Cambridge, UK (2012).
- [3] D. Tong, X. Zhang, and X. Zhang, Unsteady helical flows of a generalized oldroyd-b fluid, *Journal of non-newtonian fluid mechanics* **156**, 75 (2009).
- [4] A. Jaiswal and V. Roy, Relativistic hydrodynamics in heavy-ion collisions: general aspects and recent developments, *Adv. High Energy Phys.* **2016**, 9623034 (2016), arXiv:1605.08694 [nucl-th].
- [5] A. M. Anile, *Relativistic fluids and magneto-fluids*, *Relativistic Fluids and Magneto-fluids* (2005).
- [6] P. Kovtun, D. T. Son, and A. O. Starinets, Holography and hydrodynamics: Diffusion on stretched horizons, *Journal of High Energy Physics* **2003**, 064 (2003).
- [7] A. Lucas and K. C. Fong, Hydrodynamics of electrons in graphene, *Journal of Physics: Condensed Matter* **30**, 053001 (2018).
- [8] B. N. Narozhny, Electronic hydrodynamics in graphene, *Annals of Physics* **411**, 167979 (2019).
- [9] B. N. Narozhny, Hydrodynamic approach to two-dimensional electron systems, *La Rivista del Nuovo Cimento* **45**, 661 (2022).
- [10] M. J. H. Ku *et al.*, Imaging viscous flow of the Dirac fluid in graphene, *Nature* **583**, 537 (2020), arXiv:1905.10791 [cond-mat.mes-hall].
- [11] G. Varnavides, A. S. Jermyn, P. Anikeeva, C. Felser, and P. Narang, Electron hydrodynamics in anisotropic materials, *Nature communications* **11**, 4710 (2020).
- [12] E. H. Hasdeo, J. Ekström, E. G. Idrisov, and T. L. Schmidt, Electron hydrodynamics of two-dimensional anomalous hall materials, *Phys. Rev. B* **103**, 125106 (2021).
- [13] A. Hui, V. Oganessian, and E.-A. Kim, Beyond ohm's law: Bernoulli effect and streaming in electron hydrodynamics, *Phys. Rev. B* **103**, 235152 (2021).
- [14] X. Huang and A. Lucas, Electron-phonon hydrodynamics, *Phys. Rev. B* **103**, 155128 (2021).
- [15] O. Tavakol and Y. B. Kim, Artificial electric field and electron hydrodynamics, *Phys. Rev. Res.* **3**, 013290 (2021).
- [16] D. Di Sante, J. Erdmenger, M. Greiter, I. Matthaikakakis, R. Meyer, D. Rodríguez Fernández, R. Thomale, E. van Loon, and T. Wehling, Turbulent hydrodynamics in strongly correlated Kagome metals, *Nature Commun.* **11**, 3997 (2020), arXiv:1911.06810 [cond-mat.str-el].
- [17] B. N. Narozhny, I. V. Gornyi, and M. Titov, Hydrodynamic collective modes in graphene, *Phys. Rev. B* **103**, 115402 (2021).
- [18] J. A. Sulpizio, L. Ella, A. Rozen, J. Birkbeck, D. J. Perello, D. Dutta, M. Ben-Shalom, T. Taniguchi, K. Watanabe, T. Holder, *et al.*, Visualizing poiseuille flow of hydrodynamic electrons, *Nature* **576**, 75 (2019).
- [19] P. Gallagher, C.-S. Yang, T. Lyu, F. Tian, R. Kou, H. Zhang, K. Watanabe, T. Taniguchi, and F. Wang, Quantum-critical conductivity of the dirac fluid in graphene, *Science* **364**, 158 (2019).
- [20] A. I. Berdyugin, S. G. Xu, F. M. D. Pellegrino, R. K. Kumar, A. Principi, I. Torre, M. B. Shalom, T. Taniguchi, K. Watanabe, I. V. Grigorieva, M. Polini, A. K. Geim, and D. A. Bandurin, Measuring hall viscosity of graphene's electron fluid, *Science* **364**, 162 (2019), <https://www.science.org/doi/pdf/10.1126/science.aau0685>.
- [21] L. Ella, A. Rozen, J. Birkbeck, M. Ben-Shalom, D. Perello, J. Zultak, T. Taniguchi, K. Watanabe, A. K. Geim, S. Ilani, *et al.*, Simultaneous voltage and current density imaging of flowing electrons in two dimensions, *Nature nanotechnology* **14**, 480 (2019).
- [22] D. A. Bandurin, A. V. Shytov, L. S. Levitov, R. K. Kumar, A. I. Berdyugin, M. Ben Shalom, I. V. Grigorieva, A. K. Geim, and G. Falkovich, Fluidity onset in graphene, *Nature communications* **9**, 4533 (2018).
- [23] B. A. Braem, F. M. D. Pellegrino, A. Principi, M. Rössli, C. Gold, S. Hennel, J. V. Koski, M. Berl, W. Dietsche, W. Wegscheider, M. Polini, T. Ihn, and K. Ensslin, Scanning gate microscopy in a viscous electron fluid, *Phys. Rev. B* **98**, 241304 (2018).
- [24] A. Jaoui, B. Fauque, C. W. Rischau, *et al.*, Departure from the Wiedemann-Franz law in WP2 driven by mismatch in T-square resistivity prefactors, *npj Quant Mater* **3** **64** (2018).
- [25] P. J. W. Moll, P. Kushwaha, N. Nandi, B. Schmidt, and A. P. Mackenzie, Evidence for hydrodynamic electron flow in *pdcO₂*, *Science* **351**, 1061 (2016), <https://www.science.org/doi/pdf/10.1126/science.aac8385>.

- [26] J. Crossno, J. K. Shi, K. Wang, X. Liu, A. Harzheim, A. Lucas, S. Sachdev, P. Kim, T. Taniguchi, K. Watanabe, T. A. Ohki, and K. C. Fong, Observation of the dirac fluid and the breakdown of the wiedemann-franz law in graphene, *Science* **351**, 1058 (2016), <https://www.science.org/doi/pdf/10.1126/science.aad0343>.
- [27] D. A. Bandurin, I. Torre, R. K. Kumar, M. B. Shalom, A. Tomadin, A. Principi, G. H. Auton, E. Khestanova, K. S. Novoselov, I. V. Grigorieva, L. A. Ponomarenko, A. K. Geim, and M. Polini, Negative local resistance caused by viscous electron backflow in graphene, *Science* **351**, 1055 (2016), <https://www.science.org/doi/pdf/10.1126/science.aad0201>.
- [28] A. C. Neto, F. Guinea, N. M. Peres, K. S. Novoselov, and A. K. Geim, The electronic properties of graphene, *Reviews of modern physics* **81**, 109 (2009).
- [29] In the present article, we will assume equivalence role of Fermi energy and chemical potential, which are also considered as a temperature independent parameter but the real system may have a slight deviation from this assumptions.
- [30] N. Si, F. Zhang, W. Jiang, and Y.-L. Zhang, Magnetic and thermodynamics properties graphene monolayer with defects, *Physica A: Statistical Mechanics and its Applications* **510**, 641 (2018).
- [31] A. Boumali, Thermodynamic properties of the graphene in a magnetic field via the two-dimensional dirac oscillator, *Physica Scripta* **90**, 045702 (2015).
- [32] J. S. Ardenghi, P. Bechthold, E. Gonzalez, P. Jasen, and A. Juan, Statistical repulsion/attraction of electrons in graphene in a magnetic field, *Physica B: Condensed Matter* **433**, 28 (2014).
- [33] O. Vafek, Anomalous thermodynamics of coulomb-interacting massless dirac fermions in two spatial dimensions, *Physical review letters* **98**, 216401 (2007).
- [34] D. E. Sheehy and J. Schmalian, Quantum critical scaling in graphene, *Physical Review Letters* **99**, 226803 (2007).
- [35] D. Elias, R. Gorbachev, A. Mayorov, S. Morozov, A. Zhukov, P. Blake, L. Ponomarenko, I. Grigorieva, K. Novoselov, F. Guinea, *et al.*, Dirac cones reshaped by interaction effects in suspended graphene, *Nature Physics* **7**, 701 (2011).
- [36] Here, numerically from Fermi-integral function, we can realize the saturating value at $\mu \rightarrow 0$, but the analytical calculation of n at $\mu = 0$ become undefined due to $0 \times \infty$.
- [37] C. Kittel, *Introduction to solid state physics* (John Wiley & sons, inc, 2005).